Empirical scaling laws for wall-bounded turbulence deduced from direct numerical simulations

Philippe R. Spalart ◉
Boeing Commercial Airplanes, Seattle, Washington 98124, USA

Hiroyuki Abe ◉
Japan Aerospace Exploration Agency, Tokyo 182-8522, Japan

Statistical quantities in channel (Poiseuille), Couette, and pipe flow, including Reynolds stresses and their budgets, are studied for their dependence on the normalized distance from the wall y^+ and the friction Reynolds number Re_τ. Any quantity Q can be normalized in wall units, based on the friction velocity u_τ and viscosity ν, and it is accepted that the physics of fully developed turbulence in ducts leads to standard results of the type $Q^+ = f(y^+, \mathrm{Re}_\tau)$, in which $f(\ldots)$ means "only a function of," and f is different in different flow types. Good agreement between experiments and simulations is expected. We are interested in stronger properties for Q, generalized from those long recognized for the velocity, but not based on first principles. These include the law of the wall $Q^+ = f(y^+)$; the logarithmic law for velocity; and for the Reynolds-number dependence, the possibility that at a given y^+ it is proportional to the inverse of Re_τ, that is, $Q^+(y^+, \mathrm{Re}_\tau) = f_\infty(y^+) + f_{\mathrm{Re}}(y^+)/\mathrm{Re}_\tau$. This has been proposed before, also on an empirical basis, and recent work by Luchini [Phys. Rev. Lett. **118**, 224501 (2017)] for $Q \equiv U$ is of note. The question of whether the profiles are the same in all three flows, in other words, that there is a single function f_∞, is still somewhat open. We arrive at different conclusions for different Q quantities. The inverse-Re_τ dependence is successful in some cases. Its failure for some of the Reynolds stresses can be interpreted physically by invoking "inactive motion," following Townsend [*The Structure of Turbulent Shear Flow*, 2nd ed. (Cambridge University Press, Cambridge, 1976)] and Bradshaw [J. Fluid Mech. **30**, 241 (1967)], but that is difficult to capture with any quantitative theory or turbulence model. The case of the boundary layer is studied, and it is argued that a direct generalization of Re_τ is questionable, which would prevent a sound extension from the internal flows.

I. INTRODUCTION

A. General considerations

The friction Reynolds number $\mathrm{Re}_\tau (\equiv u_\tau h/\nu)$ of channel-flow direct numerical simulation (DNS) has risen from 180 to 5200 in the 30 years after the seminal work of Kim, Moin, and Moser [1], and it is legitimate to expect conclusive answers which clearly indicate the asymptotic behavior of the flow towards infinite Reynolds number. Here, Re_τ represents the ratio of the channel half-width h and the viscous length scale ν/u_τ, where $u_\tau \equiv (\tau_w/\rho)^{1/2}$ is the friction velocity, τ_w the wall shear stress, and ρ is the density of the fluid. A negative finding of the last decade has been that DNS fails to produce a logarithmic layer closely enough to determine the Kármán constant κ, say to the point of deciding on a value between 0.39 and 0.41. This constant is a key component in turbulence models. DNS results show a strong drift in the local value of the quantity $y^+(dU^+/dy^+)$ [see Fig. 1(b)],
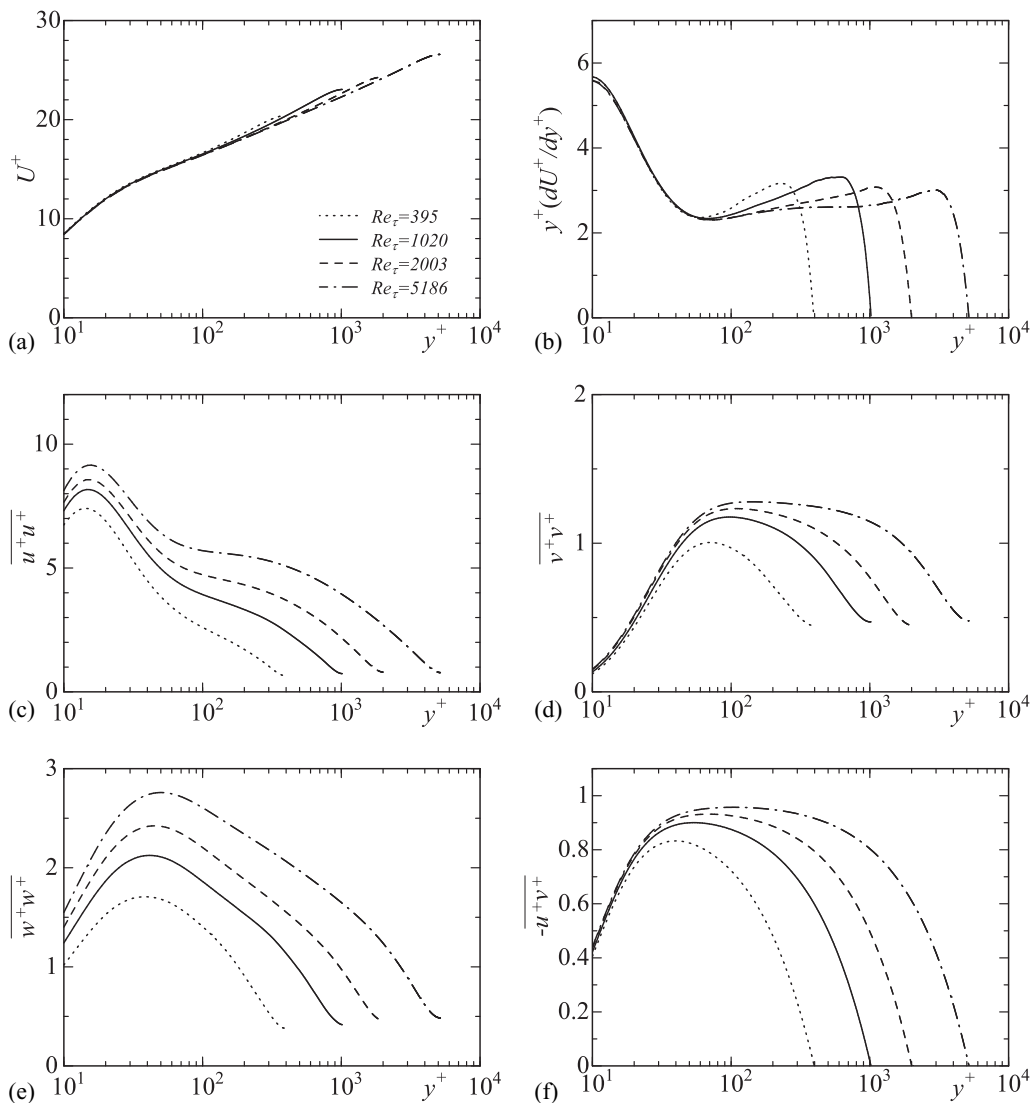
FIG. 1. Distributions of U^+, $y^+(dU^+/dy^+)$, $\overline{u^+u^+}$, $\overline{v^+v^+}$, $\overline{w^+w^+}$, $-\overline{u^+v^+}$ for channel flow for $Re_\tau = 395$ [11], 1020 [10], 2003 [12], 5186 [13]: (a) U^+; (b) $y^+(dU^+/dy^+)$; (c) $\overline{u^+u^+}$; (d) $\overline{v^+v^+}$; (e) $\overline{w^+w^+}$; (f) $-\overline{u^+v^+}$.

which ideally should be uniform and equal $1/\kappa$. It does not satisfy the expected independence on y^+, which below we name the IV property. We are basing this observation on the literature as of 2018, but a decisive increase in Reynolds number would need to be well beyond a factor of 2, so that the computing cost would increase by well over 2^4.

This situation makes Luchini's proposal attractive [2]. Much of his effort was directed at a unification between the three flows (i.e., channel, Couette, and pipe) we are considering (see [3]). The key is that he postulates a correction proportional to $1/Re_\tau$ at fixed y^+. This correction is plausible, but does not come from first principles; that would be possible only if the closure problem of turbulence had been even partially solved. Some observers would try another power of Re_τ. In Luchini's study the corrected velocity profiles come much closer to satisfying the law of the wall, hereafter denoted by LW (common to all three flows), and logarithmic properties than the

uncorrected profiles; in addition, he was able to use a single empirical constant A_1 for the three flows, which was a very favorable result. On the other hand, the corrected profiles still had too much statistical noise to deliver the value of κ, say between 0.39 and 0.41, as we envisioned; he considered that the most likely value was 0.392 based on the aggregate evidence. The success of his work for the mean velocity, always presented with scientifically rigorous warnings, led us to the idea of testing the same type of correction for other statistical quantities.

The paper by Abe and Antonia [4] used published DNS data sets for channel, pipe, and boundary layer and centered on the mean velocity U^+ and the energy dissipation rate ε^+, and particularly their integrals. The work aimed at verifying the LW and log properties, which was obtained quite closely, independently leading to the estimate $\kappa = 0.394$. The log property was linked to overlap arguments between inner and outer layers, as usual. The inner scaling established in their work for ε is indeed considered as an inverse Reynolds-number dependence here [i.e., $f_{\mathrm{Re}}(y^+)/\mathrm{Re}_\tau$]. The latter scaling yields good collapse over a wide range of Reynolds numbers for $\mathrm{Re}_\tau \geqslant 300$ and thus leads to a reasonable finite-Reynolds-number correction. They also found that for the integrals, the scaling followed the high-Reynolds-number trend even down to what are now considered low values, such as $\mathrm{Re}_\tau = 180$. These findings were another incentive to pose the same question for other quantities Q.

The charter of two recent papers (She, Chen, and Hussain [5] and Chen, Hussain, and She [6]) is far more ambitious than ours and is to provide *analytical* formulas for the velocity and Reynolds stresses in wall-bounded flows, at all Reynolds numbers. The basis is Lie groups, symmetry arguments, and random dilatations but tends to shift, and some results are recognized to be "anomalous." The approach does not agree with that of Oberlack [7], which was the pioneer for Lie groups. The empirical content of the work, as opposed to first principles, is in our opinion significant; the words "empirical parameters" are certainly used. A concrete concern is that the work appears to make the strong prediction that the value of the Kármán constant is 0.45; this is hardly tenable, based on experimental and DNS evidence.

Kaneda *et al.* [8] arrive at corrections very similar to the ones we examine here, but with a different tone: they consider the dependence $1/\mathrm{Re}_\tau$ to be motivated by theory [8]. Another recent concept in this paper and in a line of recent papers is the analogy between the Kolmogorov spectral energy cascade and a "momentum cascade" towards the wall; we consider it controversial and this belongs elsewhere.

The general question of Reynolds-number dependence in wall-bounded turbulent flows is not new, and was unavoidable in the 1988 boundary-layer DNS study of Spalart [9], which covered a factor of 4 in Reynolds number Re_{δ^*} (based on the free-stream velocity U_∞ and displacement thickness δ^*). Some of the Reynolds stresses definitely violated the LW even down to the wall. For the velocity profile, the violation of the log property was more subtle and could be blamed on "low-Reynolds-number effects" since the highest equivalent Re_τ was only in the 700 range. Boundary-layer DNS at somewhat higher Reynolds numbers is now available (and avoids the "growth terms" approximation of the 1988 study), but channel flow is a simpler situation to decipher, having a single Reynolds number, and it offers higher Re_τ values; this motivates our focus on duct flows. See the Appendix for a detailed discussion. We are fortunate that the following teams have made their DNS data available: Abe *et al.* [10,11], Hoyas and Jiménez [12], and Lee and Moser [13]. In this study, we exclusively use these DNS data sets for channel flow together with those of Pirozzoli, Bernardini, and Orlandi [14] and Avsarkisov *et al.* [15] for Couette flow and those of El Khoury *et al.* [16], Wu and Moin [17], and Ahn *et al.* [18] for pipe flow.

B. Formalization of the various conjectures

As stated in the Abstract, the starting point is $Q^+ = f(y^+, \mathrm{Re}_\tau)$ and is not a matter of debate. The first property of interest is the LW and consists in the fact that $Q^+ = f(y^+)$ only; this does not extend to the center line, that is, it requires $y \ll h$. Consequently, f may not depend on the flow type. The second property applies when $y^+ \gg 1$, and consists in the fact that Q depends on u_τ and y, but not on ν; with this reduction in the number of parameters, the dependence is dictated by dimensional

analysis, and consequently $Q^+ = f(y/h)$. This will be called IV for "independent of viscosity." The mean velocity U is widely believed to satisfy both LW and IV closely at sufficient Reynolds numbers, that is, $U^+ = f(y^+)$ from the wall up followed by $dU/dy = u_\tau/(\kappa y)$ in the logarithmic layer, but the situation for some Reynolds stresses, let alone the budgets, is far more uncertain even in the present simple flows. In terms of Reynolds-number dependence, the proposed and less well-known hyopthesis is expressed as $Q^+(y^+, \mathrm{Re}_\tau) = f_\infty(y^+) + f_{Re}(y^+)/\mathrm{Re}_\tau$, and "inverse Reynolds-number dependence" or IRD will be our notation. The question of whether the IRD requires $y \ll h$ is open. Even when IRD is verified, the question is open whether f_∞ and f_{Re} are the same in different flows, and f_{Re} often is not. Given data at two Reynolds numbers, the IRD allows an extrapolation to infinite Reynolds number, providing f_∞ and denoted by LE for linear or Luchini extrapolation. DNS evidence shown below is that the shear and wall-normal stresses, thus extrapolated, satisfy IV, in other words, within the layer having constant total shear stress, they are both constant and furthermore agree among the three flows; in other words, $Q^+ = f(-) = $ constant once $y^+ \gg 1$. In contrast, the other two stresses $\overline{u^2}$ and $\overline{w^2}$ violate, in turn, LW, no matter how small y^+ is, IRD, and IV. Their budgets also violate LW, even at the wall. The production terms since their variations are minimal fail to explain many of the observed effects, which therefore are puzzling if turbulence is approached via the local Reynolds-stress transport equation.

The paper proceeds by testing the various conjectures in order of assertiveness and in order of different moments of the turbulence, when possible on all three flows. It will appear that the conjectures work for some quantities and not others, and the unification of the three flows sought by Luchini [2,3] is far from complete. A discussion follows, including the value of the inactive motion concepts (Townsend [19]; Bradshaw [20]), and the great challenge of the textbook approach to turbulence via the moment equations; the closure problem is not new. In the Appendix, we take up the case of the boundary layer.

II. RESULTS

A. Raw statistical quantities

Figure 1 vividly illustrates the questions we are posing, using channel flow and not making any observations that are not already in the literature. Considering the highest Reynolds number, visually the velocity logarithmic layer extends roughly from $y^+ = 100$ to 1000, that is, the mean velocity approximately satisfies LW and IV (even though the total shear stress τ^+ drops from 1 to 0.8). However, the Reynolds stresses fail to do so over the same interval, with $\overline{w^+ w^+}$ deviating the most and also the one most suggestive of a logarithmic dependence on both y (to the right of the peak) and Re_τ. We also see that for U, the Reynolds-number dependence is nil near the wall, and independence gradually applies to higher values of y^+ with increasing Re_τ. Among the stresses, $\overline{v^+ v^+}$ and $-\overline{u^+ v^+}$ appear to have the same property, but only up to lower y^+ values than those for U^+, while $\overline{u^+ u^+}$ and $\overline{w^+ w^+}$ simply do not. They of course satisfy an $O(y^2)$ behavior towards the wall, but the coefficient in front of y^{+2} is conspicuously Reynolds-number dependent, at least for values accessible to DNS (while it is not rigorous to draw this conclusion using only values of y^+ larger than 1, as in this figure, we indeed checked the behavior for smaller values of y^+ (say, $y^+ \approx 0.1$) (the distributions are not shown here)). This Re dependence is concomitant with that on the wall value of the normalized dissipation ε^+ [4]. The wall values of the normalized pressure fluctuations and many other quantities also depend on Reynolds number. This extends findings of Spalart [9] to much higher Reynolds numbers, and that paper included indications of a logarithmic dependence on Reynolds number for various quantities. From 395 to 5186, the three steps for $\log(\mathrm{Re}_\tau)$ are 0.95, 0.67, and 0.95. The visual distances between the curves are quite similar to these numbers. Lozano-Duran and Jiménez [21] had similar evidence for the peak value of $\overline{u^+ u^+}$. This is taken up below.

Figure 1(b) details the failure mentioned above of DNS to exhibit a decisive plateau for the derivative of U^+ with respect to $\log(y^+)$. We recognize that the profile at $\mathrm{Re}_\tau = 5186$ displays a

short flat region, but visually it does not seem to extend the behavior at lower Reynolds numbers, and the "wave" could represent a residual lack of convergence. This is an opinion of the present authors. Similarly, the part of the theory known as law of the wake would expect the upper peak of this quantity, near $y/h = 0.6$, would be the same at all Reynolds numbers, but the profile at 1020 conflicts with the other three; this also resembles imperfect convergence.

B. Inverse Reynolds-number dependence

To begin testing IRD in all three flows, we picked the value $y^+ = 50$ for the paper. Finding the expected behavior at only one y^+ value is only a necessary condition, but 50 appears well positioned in view of Fig. 1 [at this y^+ location, significant attention has also been given to the LW properties of mean velocity in wall flows with more general pressure gradients (see [23,24])], and we verified that the same trends applied at 100 and 200. We considered $y^+ = 50$ as the beginning of the region with very weak (local) viscous effects, in other words, the purely turbulent region. The same is true at $y^+ = 200$, but not at $y^+ = 15$ where the turbulent kinetic energy (TKE) and its production take large values. We plot quantities versus $1/\text{Re}_\tau$ in Fig. 2 which represents a conjecture related to Luchini's but with a key difference: he used g/Re_τ, where the parameter g was 1 in channel flow, 0 in Couette flow, and 2 in pipe flow. IRD as we defined it is truly based on $-d\tau^+/dy^+$, and therefore Couette results would be expected to be flat. Figure 2 indicates linear behavior (that is, IRD) and commonality between flows within about 0.1 units for U^+ and with even tighter agreement for $\overline{v^+v^+}$ and $-\overline{u^+v^+}$, but not for $\overline{u^+u^+}$ or $\overline{w^+w^+}$. This appears to be a new observation, although based on literature data of course.

The results for U^+ with Re_τ larger than 500 come close to confirming Luchini's conjectures for the values 0, 1, and 2 for g, and for the dependence following gA_1y^+/Re_τ; this is represented by the slopes 50 ($gA_1 = 1$) and 100 ($gA_1 = 2$). Note that here we are testing a conjecture he made which is stronger than strict IRD: he postulated that for U the f_{Re} function is linear in y/h, and common to the three flows once the factor of g is applied.

In sharp contrast with U^+, the stresses $\overline{v^+v^+}$ and $-\overline{u^+v^+}$, satisfy IRD with the *same* value of g for channel and pipe flow. This will be discussed. These two stresses give a strong indication of their limit as $\text{Re}_\tau \to \infty$, but for the two wall-parallel ones in Figs. 2(c) and 2(e), guessing the limit would be daring, even though it is physically plausible that the limit is finite. It is equally curious that channel and pipe flow agree over $\overline{u^+u^+}$ and $\overline{w^+w^+}$, whereas Couette flow is so far removed from them. Finally, we observe that for $-\overline{u^+v^+}$ the slope is equal to -50, as it must at $y^+ = 50$ if the shear rate dU^+/dy^+ and therefore the viscous stress conform with the LW.

C. Linear extrapolation to infinite Re_τ

Motivated by the evidence from Fig. 2, we now examine whether LE produces, first, convincing results and, second, profiles which satisfy the IV property. For this, we use the highest two Re_τ values in channel flow, namely, 2003 [12] and 5186 [13]. Based on the "f_∞, f_{Re}" concept introduced in the Abstract, the definition of LE directly follows:

$$Q_{\text{LE}}^+(y^+) \equiv f_\infty(y^+) \equiv \frac{\text{Re}_{\tau 2}Q^+(y^+, \text{Re}_{\tau 2}) - \text{Re}_{\tau 1}Q^+(y^+, \text{Re}_{\tau 1})}{\text{Re}_{\tau 2} - \text{Re}_{\tau 1}}. \tag{1}$$

Note that this extrapolation approach is simpler than Luchini's equations (19)–(22), while having the same purpose; it also appears to produce smoother profiles. The figure naturally cannot extend past $y^+ = 2003$, and the effect of y/h reaching values not much smaller than 1 requires judgment; the plausible effective range is less than 2003. However, seeking a range that satisfies both $y^+ \gg 1$ and $y/h \ll 1$ is not unreasonable when $h^+(\equiv \text{Re}_\tau) = 2003$.

The LE appears to be at best moderately successful for the mean velocity, in that the putative plateau on $y^+(dU^+/dy^+)$ is much shorter than that on the profile at $\text{Re}_\tau = 5186$, but we have already stated the possibility that the latter plateau (with $\kappa \approx 0.385$) is fortuitous. A visual estimate of the
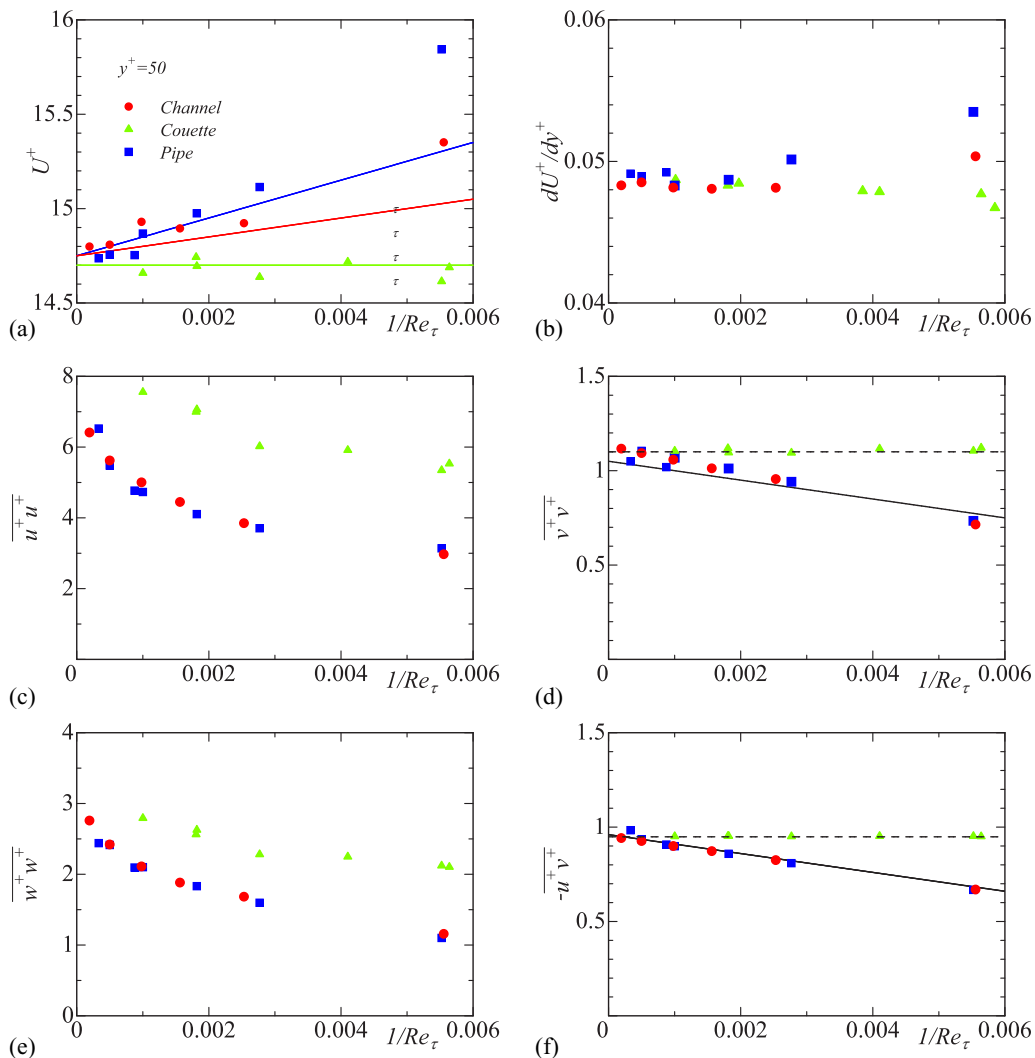
FIG. 2. Distributions of U^+, dU^+/dy^+, $\overline{u^+u^+}$, $\overline{v^+v^+}$, $\overline{w^+w^+}$, $-\overline{u^+v^+}$ for channel, Couette, and pipe flow at $y^+ = 50$ as a function of $1/\text{Re}_\tau$: (a) U^+; (b) dU^+/dy^+; (c) $\overline{u^+u^+}$; (d) $\overline{v^+v^+}$; (e) $\overline{w^+w^+}$; (f) $-\overline{u^+v^+}$. In (a), the blue, red, and yellow green lines denote the 100, 50, and 0 slopes, respectively. In (d) and (f), the solid lines denote the -75 and -50 slopes, respectively, the dashed ones the 0 slope. For channel flow (denoted as "circle"), the DNS data of [11] for $\text{Re}_\tau = 180$, 395, and 640, [10] for $\text{Re}_\tau = 1020$, [12] for $\text{Re}_\tau = 2003$, [13] for $\text{Re}_\tau = 5186$ are plotted. For Couette flow (denoted as "triangle"), the DNS data of [14] for $\text{Re}_\tau = 171$, 260, 507, and 986 and [15] for $\text{Re}_\tau = 180$, 250, and 550 are plotted. For pipe flow (denoted as "square"), the DNS data of [16] for $\text{Re}_\tau = 180$, 360, 550, and 1000, [17] for $\text{Re}_\tau = 1142$, [22] for $\text{Re}_\tau = 2003$, and [18] for $\text{Re}_\tau = 3008$ are plotted.

Kármán constant κ accounting for residual waviness over the narrow range [250,400] is roughly from 0.394 to 0.396. This is close to Luchini's 0.392 [3] [see Fig. 3(b)]. He derived his estimate from a combination of evidence between the three flows. The present κ obtained from the LE is also close to that of Abe and Antonia [4]. The latter authors obtained $\kappa = 0.394$ on the basis of the scaling argument for the energy dissipation rate in a channel, pipe, and zero-pressure-gradient boundary layer. Experimentally, Marusic *et al.* [26] reported a universal logarithmic behavior of U^+ with
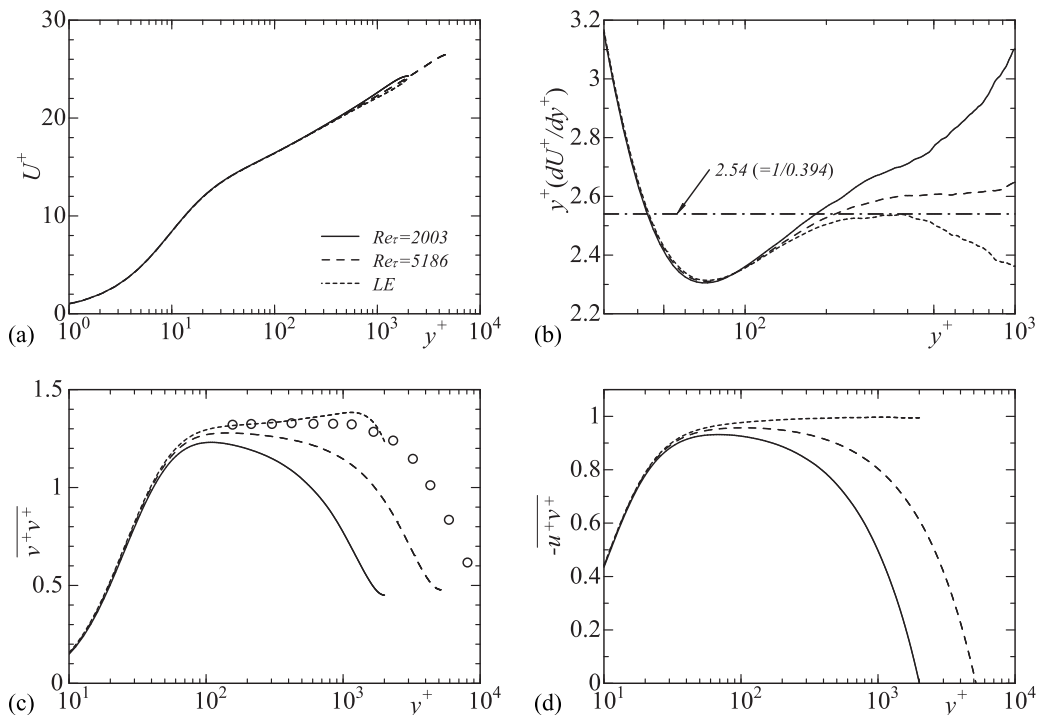
FIG. 3. Distributions of raw and extrapolated U^+, $y^+(dU^+/dy^+)$, $\overline{v^+v^+}$, and $-\overline{u^+v^+}$ to infinite Re_τ with the use of LE [relation (1)]: (a) U^+; (b) $y^+(dU^+/dy^+)$; (c) $\overline{v^+v^+}$; (d) $-\overline{u^+v^+}$. In the extrapolation, the two DNS data at $Re_\tau = 2003$ [12] and 5186 [13] are used. In (c), the circle denotes the experimental data of [25] in a pipe for $Re_\tau \approx 10^4$.

$\kappa = 0.39$ over a wide range of Reynolds number (i.e., $Re_\tau = 1.8 \times 10^4 \sim 6.3 \times 10^5$) by examining data sets in two laboratory boundary layers [27,28], the superpipe using the hot-wire measurement [29], and an atmospheric surface layer [30]. The log law with $\kappa = 0.39$ also provides a good fit to the distributions of U obtained from the recent CICLoPE pipe experiment up to $Re_\tau = 4 \times 10^4$ (see Örlü *et al.* [31]).

We note that several authors with somewhat different tools to exploit the DNS evidence in three flows all arrive at values for the Kármán constant between 0.39 and 0.40; this is outside the relatively well-established bracket, which was 0.40 to 0.41 until roughly the year 2000. Importantly, high-Reynolds-number pipe experiments point at values approaching 0.42 (McKeon *et al.* [32]), also using different tools involving the center-line velocity, so that the uncertainty in the community over κ subsists (see also Marusic *et al.* [26] who examined the uncertainty of κ in their work and arrived at $\kappa = 0.39 \pm 0.02$).

The behavior of $-\overline{u^+v^+}$ after LE is as expected, strongly following IV and of course approaching 1. The LE makes it equal $1 - dU^+/dy^+$, and dU^+/dy^+ is both well behaved and very small for large y^+. The other stress $\overline{v^+v^+}$, after LE, rises when approaching the channel center line. This can be attributed to "center-region effects" (meaning that we do not have $y/h \ll 1$), and the same figure but for LE based on Re_τ of 1020 and 5186 is consistent with this. We estimate that the IV value for $\overline{v^+v^+}$ in f_∞ can be taken from the region near $y^+ = 200$, and is close to 1.33. The latter value agrees well with the measurement of Zhao and Smits [25] in a pipe flow at $Re_\tau \approx 10^4$ (see Fig. 3 where the LE distribution shows a near plateau above $y^+ = 200$ and is essentially identical with that of [25]). We have also tested LE for Couette and pipe flow, using DNS data albeit at lower Reynolds
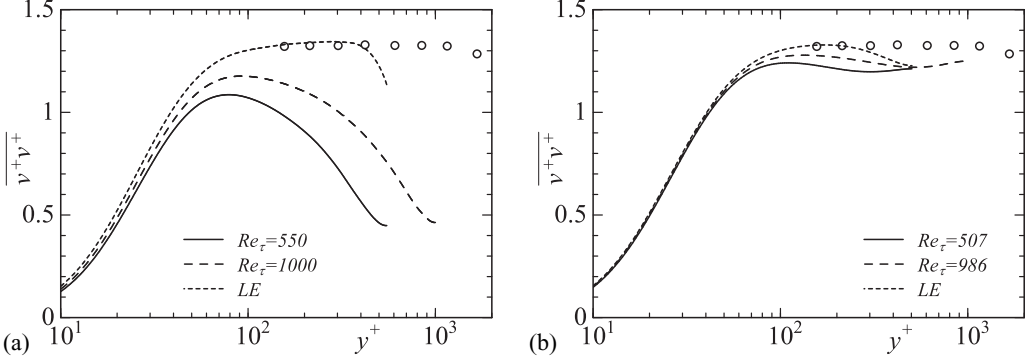
FIG. 4. Distributions of extrapolated $\overline{v^+v^+}$ to infinite Re_τ with the use of LE [relation (1)] for Couette and pipe flow: (a) pipe flow; (b) Couette flow. In the extrapolation, the two DNS data at $\mathrm{Re}_\tau = 550$ and 1000 [16] are used for pipe flow, whereas those at $\mathrm{Re}_\tau = 507$ and 986 [15] are used for Couette flow. The circle denotes the experimental data of [25] in a pipe for $\mathrm{Re}_\tau \approx 10^4$.

numbers than those for channel flow (see Fig. 4). Indeed, LE produces the IV property adequately for the active motion, i.e., $\overline{v^+v^+} \approx 1.3$ and $-\overline{u^+v^+} \approx 1$ (the distribution of $-\overline{u^+v^+}$ for Couette and pipe flow is not shown) at $y^+ \geqslant 200$.

D. Reynolds-stress budgets

Figure 5 examines the Reynolds-number dependence in channel flow for budgets, in a search for a physical understanding of Figs. 1(c) to 1(f). The transport equation of $\overline{u_i^+ u_j^+}$ is defined such that

$$0 = P_{ij}^+ + T_{ij}^+ + \Pi_{ij}^+ + D_{ij}^+ - \varepsilon_{ij}^+, \tag{2}$$

where

$$P_{ij}^+ = -\overline{u_j^+ u_k^+}(\partial \overline{U}_i^+/\partial x_k^+) - \overline{u_i^+ u_k^+}(\partial \overline{U}_j^+/\partial x_k^+), \tag{3}$$

$$T_{ij}^+ = -\partial(\overline{u_i^+ u_j^+ u_k^+})/\partial x_k^+, \tag{4}$$

$$\Pi_{ij}^+ = -\overline{u_j^+(\partial p^+/\partial x_i^+)} - \overline{u_i^+(\partial p^+/\partial x_j^+)}, \tag{5}$$

$$D_{ij}^+ = \partial^2(\overline{u_i^+ u_j^+})/\partial x_k^{+2}, \tag{6}$$

$$\varepsilon_{ij}^+ = 2\overline{(\partial u_i^+/\partial x_k^+)(\partial u_j^+/\partial x_k^+)}. \tag{7}$$

$P_{ij}^+, T_{ij}^+, \Pi_{ij}^+, D_{ij}^+, \varepsilon_{ij}^+$ denote the production, turbulent diffusion, velocity-pressure gradient correlation, molecular diffusion, and homogeneous dissipation, respectively.

The findings in Fig. 5 may be simplest to describe for $\overline{u^+u^+}$: the production term is very well behaved [its maximum value also approaches 0.5 (the theoretical maximum value) as Re_τ increases], which is crucial as it is the only external term locally, and is also the production term for the entire turbulent kinetic energy. In other words, production differences do nothing to explain the differences in Fig. 1(c). The most vivid effect here is on the near-wall molecular diffusion and dissipation (as fully predicted by Bradshaw in 1967 [20], although he was varying an adverse pressure gradient rather than the Reynolds number). These two viscous terms largely cancel. This would argue in favor of modeling them together but that would, first, remove the common assumption that dissipation is always a loss term, and second remove the numerical advantage of having a diffusion term, which moreover is exact. The near-wall values are fairly consistent with a logarithmic dependence on Re_τ,
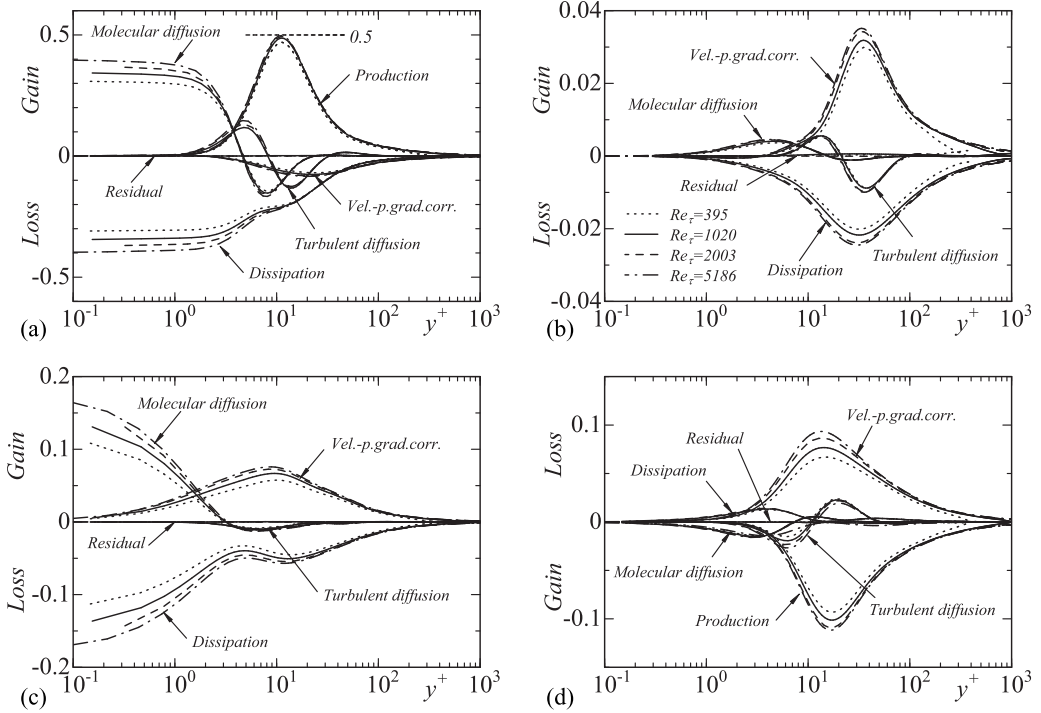
FIG. 5. Budgets of Reynolds stresses normalized by u_τ^4/ν for channel flow at $\mathrm{Re}_\tau = 395$ [11], 1020 [10], 2003 [12], $\mathrm{Re}_\tau = 5186$ [13]: (a) $\overline{u^+u^+}$; (b) $\overline{v^+v^+}$; (c) $\overline{w^+w^+}$; (d) $\overline{u^+v^+}$.

but this is not our focus. The pressure term has a definite trend, but it will be easier to see in the budgets of the other stresses.

The budget of $\overline{w^+w^+}$ has the same trends as that of $\overline{u^+u^+}$ for the viscous terms. Its primary gain term, from pressure, strongly increases with Reynolds number, this being offset by dissipation. A Reynolds-stress model with a return-to-isotropy component could capture this trend, driven by the rapid increase of $\overline{u^+u^+}$ in Fig. 1(c) but only if, precisely, it had first captured the behavior of $\overline{u^+u^+}$.

The behavior of the budgets of $\overline{v^+v^+}$ and $-\overline{u^+v^+}$ displays somewhat unexpected trends, considering the resilience of the stresses themselves in Fig. 1, but notice the much expanded vertical scales. The gain term of $-\overline{u^+v^+}$ which is proportional to $\overline{v^+v^+}$ has a definite increase at higher Re_τ, more than offset by an increase of the pressure term. The identical increase in the gain term of $-\overline{u^+v^+}$ as Re_τ increases is observed for pipe flow, but not for Couette flow (see Fig. 6 where the data of $-P_{12}^+$ at $y^+ = 50$ are plotted as a function of $1/\mathrm{Re}_\tau$ for the three flows). This result is consistent with the IRD of $-\overline{u^+v^+}$ [see Fig. 2(f)]. At first sight, this will be very challenging to model. As for $\overline{v^+v^+}$, the pressure term and the opposing dissipation have fairly strong variations, but for both stresses there is a tendency to saturate between Re_τ of 2003 and 5186; in other words, we see no evidence of a continuing logarithmic dependence on Re_τ (the exception is the pressure term for $-\overline{u^+v^+}$).

Overall, except for the near-wall viscous terms, the Reynolds-number dependence of the budgets is, maybe surprisingly, weaker than the dependence of the stresses themselves in Fig. 1, especially when it comes to $\overline{w^+w^+}$. The guidance in terms of the expected "dialogue" between stresses and budgets, needed to make substantial progress in modeling, is unfortunately not clear to us. As mentioned, the local term-by-term "mechanisms" in conventional models are fully compatible with solutions which satisfy LW and IV, and in such models the effect of the distance to the center line expressed in wall units, i.e., Re_τ, is weak indeed.
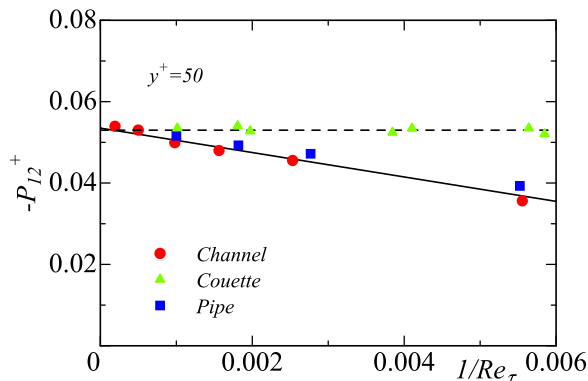
FIG. 6. Distributions of $-P_{12}^+$ for channel, Couette, and pipe flow at $y^+ = 50$ as a function of $1/\text{Re}_\tau$. The solid and dahed lines denote the -3 and 0 slopes, respectively. For channel flow (denoted as "circle"), the DNS data of [11] for $\text{Re}_\tau = 180$, 395, and 640, [10] for $\text{Re}_\tau = 1020$, [12] for $\text{Re}_\tau = 2003$, [13] for $\text{Re}_\tau = 5186$ are plotted. For Couette flow (denoted as "triangle"), the DNS data of [14] for $\text{Re}_\tau = 171$, 260, 507, and 986 and [15] for $\text{Re}_\tau = 180$, 250, and 550 are plotted. For pipe flow (denoted as "square"), the DNS data of [16] for $\text{Re}_\tau = 180$, 360, 550, and 1000 are plotted.

III. DISCUSSION, TURBULENCE MODELING, AND FUTURE WORK

We have formulated as clearly as we could and tested a variety of conjectures regarding the statistics of channel, Couette, and pipe flow, with emphasis on Reynolds-number and flow-type dependence. The findings are unfortunately not simple, as the quantities separate into at least three classes. First, the mean velocity U^+ is most probably well behaved, as found by Luchini [2,3], but its Reynolds-number dependence at a given y^+ value differs by a factor of approximately 2 between channel and pipe flow. Second, the Reynolds stresses $\overline{v^+v^+}$ and $-\overline{u^+v^+}$ are well behaved, but without the factor of 2. Third, the stresses $\overline{u^+u^+}$ and $\overline{w^+w^+}$ are poorly behaved, although only as judged by the simple conjectures we introduced. Again, these do not originate in first principles or exact moment equations of turbulence.

As mentioned, Luchini [2,3] obtained his factor of 2 in the pipe by invoking dP^+/dx^+ rather than $d\tau^+/dy^+$. In general, we object to the pressure gradient proper in turbulence theories and models (see Spalart and Speziale [33]) because this term has no local effect on vorticity, and we believe terms derived from Reynolds stresses are more convincing. Actually, this is possible since in a steady flow $dP/dx = \partial \tau_{i1}/\partial x_i$, which equals $2\partial \tau/\partial y$ in the axisymmetric flow; this has been called the "turbulence force." This argument removes a theoretical objection to the factor of 2. Other interpretations also lessen the conflict, as illustrated in Fig. 7. The shear stress is $-\overline{u^+v^+}$, but the momentum flux across the surface at y is $-(1 - y/R)\overline{u^+v^+}$, where R is the radius of curvature of the wall (therefore, infinite in the plane flows). This quantity is shown in Fig. 7(a), and the difference between the pipe-flow curve and 1 is roughly double the difference between the channel-flow curve and 1; in other words, the behavior is similar to that of the velocity U^+ in Fig. 2(a). The effect of cylindrical coordinates on the mean pressure is similar, as seen in Fig. 7(b). Again, pipe flow strongly raises the effect relative to channel flow; this is because the mean momentum equation dictates that $P^+ = -\overline{v^+v^+} + \int (\overline{w^+w^+} - \overline{v^+v^+})/r\,dr + c$, where $r \equiv R - y$ and c is an arbitrary constant. This underlines the impact of differences between the normal Reynolds stresses. Note that $\overline{w^+w^+} - \overline{v^+v^+}$ depends on Re_τ, so that the difference between the two flows is not a simple function, and certainly not a simple factor of 2.

This leaves the third class of quantities, namely, $\overline{u^+u^+}$ and $\overline{w^+w^+}$. The theories of inactive motion are convincing in addressing the Reynolds-number trends, but exceed the reach of the simple conjectures we have tested here. In particular, there are strong hints that major quantities such as the peak Reynolds stress $\overline{u^+u^+}_{max}$, the wall dissipation rate ε_w^+, the wall pressure intensity $\overline{p_w^+ p_w^+}$,
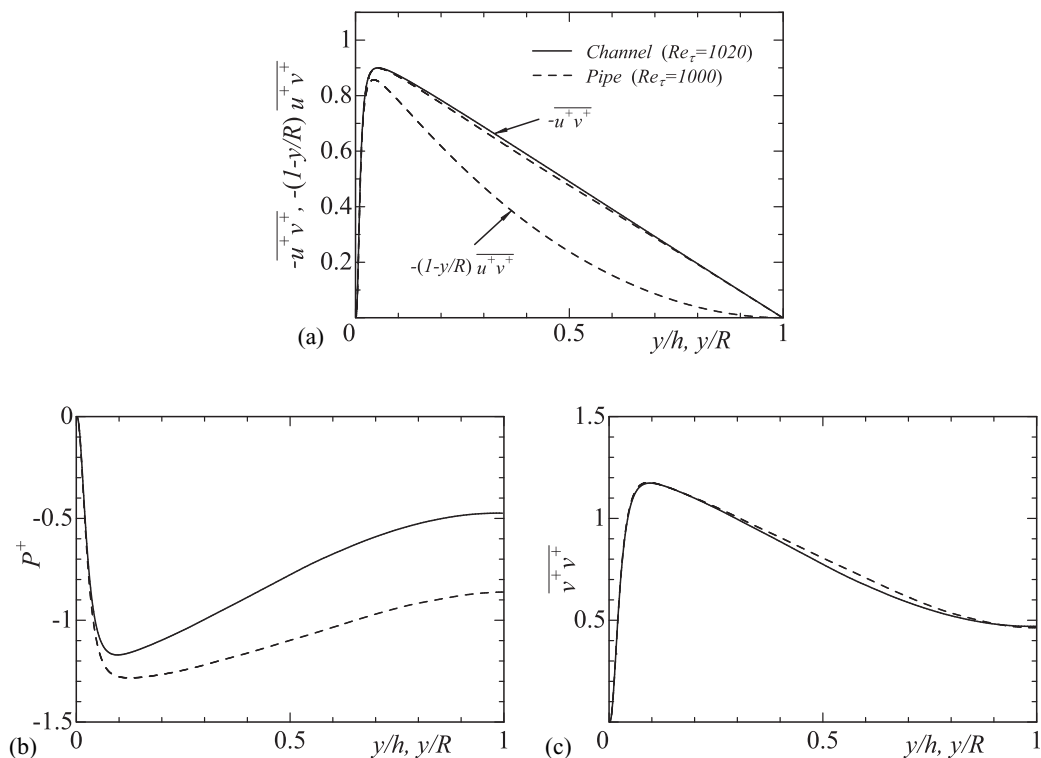
FIG. 7. Distributions of $-\overline{u^+v^+}$, $-(1-y/R)\overline{u^+v^+}$, P^+, and $\overline{v^+v^+}$ for channel and pipe flow at $\mathrm{Re}_\tau = 1020$ [10] and 1000 [16]: (a) $-\overline{u^+v^+}$, $-(1-y/R)\overline{u^+v^+}$; (b) P^+; (c) $\overline{v^+v^+}$.

and others have a logarithmic dependence on Reynolds number, in the DNS range for Re_τ. This is radically different from the inverse Reynolds-number dependence Luchini and we have introduced for other quantities, and raises the possibility that their limit as $\mathrm{Re}_\tau \to \infty$ is not finite, which may appear paradoxical. This is the limit in wall units, and it is yet possible that the limit, when normalized with the center-line velocity in a duct or the edge velocity of a boundary layer, is finite or even zero. There is conflicting evidence of this since the peak value of $\overline{ww}$, normalized by the center-line velocity squared, varies only from 0.0040 to 0.0038 as deduced from Fig. 1 but the same test for $\overline{uu}$ yields 0.0176 and 0.0128, a much larger difference. Conjectures comparable in simplicity to the present ones, but able to render inactive motion, may be proposed in the future, but a role for the center-line velocity is not consistent with classical (local) arguments.

A. Turbulence modeling

The findings presented here are quite relevant to turbulence modeling because in our opinion the analytical structure of conventional turbulence models naturally leads them to obey both LW and IV. Gross disagreements of RANS with DNS for $\overline{u^+u^+}$ and $\overline{w^+w^+}$ are widespread, and mere adjustments of constants in the models will be powerless against this. This observation is not new at all. Bradshaw [20,34] explicitly suggested "modeling only the active part of the turbulence," and both Saffman and Wilcox have written similar comments. This posits the idea of a hypothetical turbulence model, requiring a scientific endeavor which could involve two successive steps: first, declaring the profiles of the newly conceived active Reynolds stresses, all the way across the y^+ range, satisfying both LW and IV; second, creating the partial differential equations (PDE) which
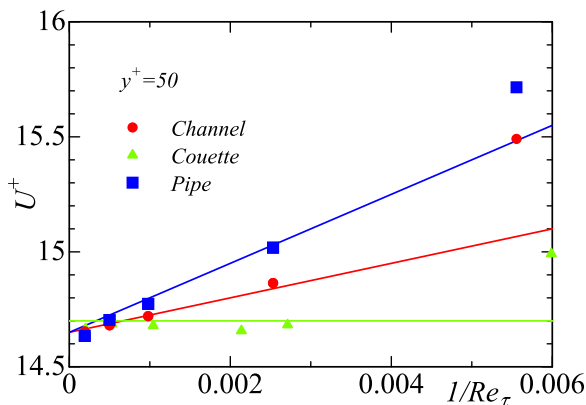
FIG. 8. Distributions of U^+ predicted with the use of the SA model [36] for channel, Couette, and pipe flow at $y^+ = 50$ as a function of $1/\text{Re}_\tau$. The blue, red, and yellow green lines denote the 150, 75, and 0 slopes, respectively. For channel flow (denoted as "circle"), the calculations have been made at $\text{Re}_\tau = 180, 395, 1020, 2000,$ and 5200. For Couette flow (denoted as "triangle"), the calculations have been made at $\text{Re}_\tau = 167, 369, 468, 959, 1886,$ and 4927. For pipe flow (denoted as "square"), the calculations have been made at $\text{Re}_\tau = 180, 395, 1020, 2000,$ and 5200.

produce these profiles, so as to have a usable RANS model. Both steps are very arduous; we know of no quantitative proposal even for the first one. We are envisioning an argument leading to a unique result, even if it applies only to the plateaus in the log layer.

The variation of the viscous shear stress dU^+/dy^+ in Fig. 2(b) deserves comments, as it appears to distinguish different types of turbulence models. A direct application of mixing-length theory predicts the following dependence: $d(dU^+/dy^+)/d(1/\text{Re}_\tau) = -y^+/(2l^+)$ where l is the mixing length. Assuming that $l = \kappa y$ as is standard and $\kappa \approx 0.4$, we arrive at $d(dU^+/dy^+)/d(1/\text{Re}_\tau) \approx -1.25$. The figure shows that $d(dU^+/dy^+)/d(1/\text{Re}_\tau) \approx +0.6$. Therefore, assuming that the mixing length is insensitive to pressure gradient (here quantified by $1/\text{Re}_\tau$) gives even the wrong sign for the variation, a fact observed in DNS by Spalart and Watmuff [23] and very much confirmed in both favorable and adverse pressure gradients by Johnstone *et al.* [24]. Luchini [35] has made very similar observations.

Models based on transport PDEs do not behave like the mixing-length model. Figure 8, applying the Spalart-Allmaras (SA) model [36], can be compared with Fig. 2(a). The mean velocity U^+ at $y^+ = 50$ now increases when Re_τ decreases, and correctly orders Couette, channel, and pipe flow. The slope is incorrect, being roughly $\frac{3}{2}$ times that of DNS, but this is still a limited success. It appears that the global nature of the PDE solution in the full domain (as opposed to the local nature of the mixing-length model) injects the relatively subtle effect of Re_τ at $y^+ = 50$ with the correct sign, and a magnitude which is not grossly inaccurate. In future work, the IRD will also be examined for two-equation turbulence models [i.e., $k - \varepsilon$ and Menter's shear stress transport (SST) models]. Note that the IRD property is quite natural for turbulence models, whether mixing length or PDE based, considering the dominant role of the shear stress, of which the gradient is proportional to $1/\text{Re}_\tau$.

Anecdotally, turbulence models exist with known IV properties (plateaus) in the log layer. The SSG-LRR-ω model [37] yields $\overline{u^+u^+} = 2.9$, $\overline{v^+v^+} = 1.4$, $\overline{w^+w^+} = 2.1$ whereas the SA-QCR2013 model [38] yields $\overline{u^+u^+} = 2.7$, $\overline{v^+v^+} = 1.5$, $\overline{w^+w^+} = 2.1$ [see turbulence modeling resource (TMR) website [39]]. For the SA model, the turbulent kinetic energy k is sometimes estimated by using the approximation $\nu_t\sqrt{2S_{ij}S_{ij}}/a_1$, where a typical value for a_1 is 0.31. Here, this approximation is made solely for visualizing the normal stresses (it is not done while solving

the Navier-Stokes equations) (see also [40]). The Reynolds-stress model (RSM) is definitely more accurate, especially for $\overline{v^+v^+}$, since above we propose the value 1.33. The quadratic constitutive relation (QCR) model was optimized for the outer part of the boundary layer, where the anisotropy is weaker; it is also a much simpler model.

B. Active turbulence

There are at least two incentives to define "active turbulence." The first is understanding and clarity in our knowledge of near-wall turbulence, and was pursued by Townsend [19], Bradshaw [20], and others. The second is practical: Would such a model not render all of the turbulence, but still make a sufficiently accurate contribution to the momentum equation? Channel flow provides an extreme situation: the nonuniversal stresses $\overline{u^+u^+}$ and $\overline{w^+w^+}$ simply do not enter the momentum equation. They also have a very weak effect on a boundary layer without pressure gradient. However, this is not true anymore with strong pressure gradients, and corner flows also are very sensitive to differences between the six stresses. We cannot propose a model that is "fully competent" in channel flow, and channel flow alone.

Future work may produce concrete conjectures similar to those tested here that capture the behavior of $\overline{u^+u^+}$ and $\overline{w^+w^+}$, presumably including the relatively well-accepted logarithmic dependence on y in the neighborhood of $y/h = 0.1$, and an unknown dependence on Re_τ. It seems that the available corpus of DNS data is sufficient for this purpose, but creativity will be needed. A better theoretical understanding of the g factor between channel and pipe flow would be most welcome. The cause of the lower U^+ values produced by Couette flow DNS [14] (see [3]) needs to be explored; it is possible some numerical aspects are responsible, and new DNS with a finer grid at a moderate Reynolds number will not be difficult (although domain-size effects reported by Tsukahara *et al.* [41] and Gandía-Barberá *et al.* [42] are troublesome in this flow). Now, Couette flow is prone to develop global streamwise vortices in the center region of the channel. Gandía-Barberá *et al.* [42] reported that the length and width of the rolls are approximately $50h$ and $2.5h$, respectively, for $\mathrm{Re}_\tau \approx 130$. At first sight, this should have very little impact at $y^+ = 50$ when $\mathrm{Re}_\tau = 1000$, but the global vortices are an extreme type of inactive motion, and Fig. 2(c) shows vastly higher values of $\overline{u^+u^+}$ and $\overline{w^+w^+}$ in Couette flow than in the other two. Together, Figs. 2(c)–2(e) indeed show that the correlation coefficient between u and v, which is an aspect of the "structure" of the turbulence, is significantly lower in Couette flow.

IV. CONCLUSIONS

Unquestionably, the assumptions of universal behavior which turbulence theory and modeling rest on are never fully secure, even in the present very simple flows. The removal of experimental uncertainty by DNS, leading to near perfection for simple geometries over a fairly wide range of Reynolds number, and the attendant expectation for high precision seem to first and foremost clarify the (partial) failures of the theory. On the other hand, the evidence of success for the inverse Reynolds-number dependence (IRD) of several quantities is a positive result, which appears even for the log layer when Re_τ is finite. Indeed, the active motion (i.e., $\overline{vv}$ and $\overline{uv}$) follows the IRD excellently for the three flows, which in the case of $\overline{uv}$ is intrinsically linked to the IRD of U. Also, we have proposed the linear extrapolation (LE) to infinite Reynolds number of a quantity Q on the basis of the IRD; the resulting relation (1) successfully predicts the extremely large Reynolds-number behaviors (i.e., $\kappa \approx 0.394$ and $\overline{v^+v^+} \approx 1.3$). Our analysis indicates that for the three flows, the value of f_∞ in the law of the wall $Q^+ = f(y^+)$ remains intrinsically unchanged for the active motion, while that of $f_{\mathrm{Re}}(y^+)$ depends on the total shear stress τ.

To summarize, this study appears to clarify only some aspects of wall-bounded turbulence. The logical next step, namely extending theory and modeling to relevant flows with varied pressure gradients and three dimensionality, will be an even greater challenge.

APPENDIX: CASE OF THE BOUNDARY LAYER

The boundary layer shares the essential near-wall physics of turbulence with the three internal flows we explored in this paper. Our reason for not including it across the paper is that in our opinion a Reynolds number equivalent to Re_τ is not available, so that the IRD conjecture cannot be formulated with rigor.

In Fig. 9, we present a subset of the quantities displayed in Fig. 1, using DNS data of a zero-pressure-gradient turbulent boundary layer (TBL) made available by Spalart [9], Schlatter and Örlü [45], Jiménez *et al.* [44], Sillero *et al.* [46], and Abe [43]. The figures confirm the close agreement on the mean velocity U^+ from various sources [Fig. 9(a)], the smooth rise of $\overline{v^+v^+}$ with Reynolds number apparently to a high-Reynolds-number asymptote [Fig. 9(d)], and the less regular behavior of $\overline{u^+u^+}$ with uncertain behavior for its peak value [Fig. 9(c)]. We note the vigorous theoretical and experimental work devoted recently to ascertaining whether as the Reynolds number rises to ∞, the peak value *in wall units* rises without limit or asymptotes to a finite level (Monkewitz [47]; Chen and Sreenivasan [48]). This is a question we left fully open here. There is no doubt the same
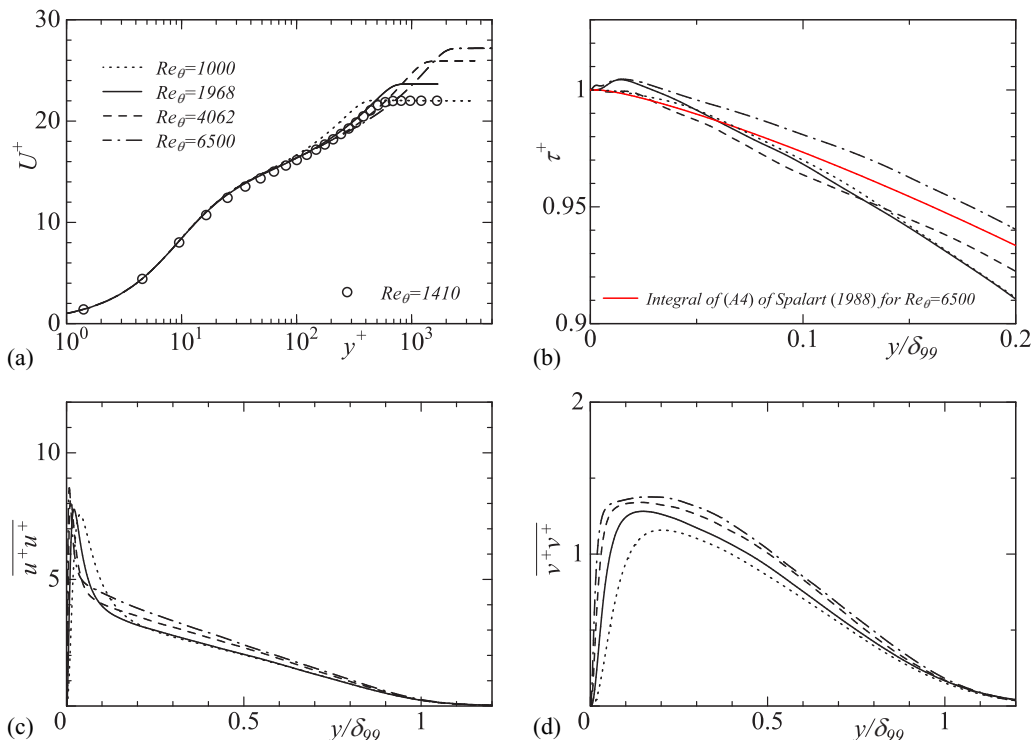

FIG. 9. Distributions of U^+, τ^+, $\overline{u^+u^+}$, and $\overline{v^+v^+}$ for TBL for $Re_\theta = 1000$ [43], 1968 [44], 4062 [45], and 6500 [46]: (a) U^+; (b) τ^+; (c) $\overline{u^+u^+}$; (d) $\overline{v^+v^+}$. In (a), the circle denotes the DNS data of [9] for $Re_\theta = 1410$. In (b), the red line denotes the integral of Eq. (A4) of Spalart [9] [or, equivalently, (A1) of this paper] for $Re_\theta = 6500$ [46]. Note that δ_{99} denotes the 99% boundary-layer thickness.

authors have a similar interest in the internal flows. Aside from the peak of $\overline{u^+u^+}$, quantities such as the wall dissipation ϵ^+ and the pressure rms p^+_{rms} open the same question, with the pressure rms quite important in practice for aircraft cabin noise. It rises logarithmically with Reynolds numbers at DNS-accessible Reynolds numbers [see Fig. 14 of Spalart [9]; Fig. 7(b) of Sillero *et al.* [46]], a fact which is compatible with the attached-eddy hypothesis (Townsend [19]), but the ultimate trend is not known.

The boundary layer has many possible definitions for its thickness: displacement thickness δ^*; momentum thickness θ; and then competing definitions for the full thickness δ, either by the 99% or 99.5% velocity level, or integrals of the total shear stress (Spalart [9]) or of the velocity defect multiplied by U_∞/u_τ (Monkewitz [47]) which can be traced to Clauser [49].

A key point is that in the internal flows with streamwise pressure decrease, $-1/\text{Re}_\tau$ sets the slope of the total shear stress versus y^+. The TBL has no such pressure decrease, and at first sight would resemble Couette flow. However, Spalart in 1988 [9] showed that this is not compatible with the momentum equation, and derived an equation for $d\tau^+/dy$ [his (A4)] which is an exact consequence of the velocity law of the wall (an analogous relation has been proposed by Nakamura *et al.* [50] on a TBL with an adverse pressure gradient) and the slow decrease of u_τ as the streamwise distance x increases. The algebra is not immediate, and a fortuitous cancellation between UU_x and VU_y simplifies the result much, leading to a single term in (A4) [note that U and V denote the mean streamwise (x) and wall-normal (y) velocities, respectively; the subscripts denote the partial derivative]. This equation is

$$\frac{\partial\tau^+}{\partial y} = \frac{d\,\log(u_\tau)}{dx}U^{+2}. \tag{A1}$$

This was expanded by Monkewitz and Nagib [51], including a version of Spalart's (A6). Spalart showed that at higher Reynolds numbers $\partial\tau^+/\partial y$ was approximately equal to $-0.5/\delta$ with δ the full boundary-layer thickness, so that Re_τ might logically be approximately equal to $2\delta^+$. As a result, formulating the IRD rigorously is difficult since it hinges on Re_τ. This is an important consequence obtained from this analysis and highlights a discernible difference in the Re effect between the internal and external flows.

Figure 9(b) presents facts of interest. First, the slope of the stress, calculated from Spalart's (A4), agrees closely with the slope of the true stress from the DNS at the same Reynolds number over most of the region showed. This suggests that the algebra is correct [note that (A4) is valid all the way to the wall, not only in the log layer, and κ is not involved], that the DNS data set does satisfy the mean-velocity law of the wall as x increases, and that the estimates of δ are consistent. At the Reynolds numbers available today, the curves have residual curvature, and do not approach a slope of -0.5. The second fact is a spurious "ramp" in the stress for y/δ less than about 0.01 in two of the data sets; this ramp is not compatible with the momentum equation. The other two data sets are a little wavy and disagree somewhat with (A4), which suggests a lack of convergence. We are clearly approaching the limit of the quality of current DNS data sets; in other words, we are exhibiting detailed quantities which are too sensitive for the figures to appear perfect. The shape of $\overline{v^+v^+}$ at the highest Reynolds number, similarly, does not suggest a "family" the way the curves in Fig. 1(d) do.

We conclude that a firm definition of Re_τ and therefore the IRD is not today available in the boundary layer. We also note that the meaning of Spalart's (A4) and (A8) is unfortunately ignored by most of the community, which ignores the dependence of τ^+ on y. Figure 9(b) is very clear, and should be helpful in this domain.

---

[1] J. Kim, P. Moin, and R. Moser, Turbulence statistics in fully developed channel flow at low Reynolds number, J. Fluid Mech. **177**, 133 (1987).

[2] P. Luchini, Universality of the Turbulent Velocity Profile, Phys. Rev. Lett. **118**, 224501 (2017).

[3] P. Luchini, Structure and interpretation of the turbulent velocity profile in parallel flow, Eur. J. Mech. B **71**, 15 (2018).

[4] H. Abe and R. A. Antonia, Relationship between the energy dissipation function and the skin friction law in a turbulent channel flow, J. Fluid Mech. **798**, 140 (2016).

[5] Z. S. She, X. Chen, and F. Hussain, Qquantifying wall turbulence via a symmetry approach. Part 1. A Lie group theory, J. Fluid Mech. **827**, 322 (2017).

[6] X. Chen, F. Hussain, and Z. S. She, Quantifying wall turbulence via a symmetry approach. Part 2. Reynolds stresses, J. Fluid Mech. **850**, 401 (2018).

[7] M. Oberlack, A unified approach for symmetries in plane parallel turbulent shear flows, J. Fluid Mech. **427**, 299 (2001).

[8] Y. Kaneda, Y. Yamamoto, and Y. Tsuji, Linear Response Theory for One-Point Statistics in the Inertial Sublayer of Wall-Bounded Turbulence, Phys. Rev. Lett. **122**, 194502 (2019).

[9] P. R. Spalart, Direct simulation of a turbulent boundary layer up to $R_\theta = 1410$, J. Fluid Mech. **187**, 61 (1988).

[10] H. Abe, H. Kawamura, and Y. Matsuo, Surface heat-flux fluctuations in a turbulent channel flow up to $Re_\tau = 1020$ with $Pr = 0.025$ and 0.71, Int. J. Heat Fluid Flow **25**, 404 (2004).

[11] H. Abe, R. A. Antonia, and H. Kawamura, Correlation between small-scale velocity and scalar fluctuations in a turbulent channel flow, J. Fluid Mech. **627**, 1 (2009).

[12] S. Hoyas and J. Jiménez, Reynolds number effects on the Reynolds-stress budgets in turbulent channels, Phys. Fluids **20**, 101511 (2008).

[13] M. Lee and R. D. Moser, Direct numerical simulation of turbulent channel flow up to $Re_\tau \approx 5200$, J. Fluid Mech. **774**, 395 (2015).

[14] S. Pirozzoli, M. Bernardini, and P. Orlandi, Turbulence statistics in Couette flow at high Reynolds number, J. Fluid Mech. **758**, 327 (2014).

[15] V. Avsarkisov, S. Hoyas, M. Oberlack, and J. P. G. Galache, Turbulent plane Couette flow at moderately high Reynolds number, J. Fluid Mech. **751**, R1 (2014).

[16] G. K. El Khoury, P. Schlatter, A. Noorani, P. F. Fischer, G. Brethouwer, and A. V. Johansson, Direct numerical simulation of turbulent pipe flow at moderately high Reynolds numbers, Flow Turbul. Combust. **91**, 475 (2013).

[17] X. Wu and P. Moin, A direct numerical simulation study on the mean velocity characteristics in turbulent pipe flow, J. Fluid Mech. **608**, 81 (2008).

[18] J. Ahn, J. H. Lee, J. L. Lee, J.-H. Kang, and H. J. Sung, Direct numerical simulation of a 30R long turbulent pipe flow at $Re_\tau = 3008$, Phys. Fluids **27**, 065110 (2015).

[19] A. A. Townsend, *The Structure of Turbulent Shear Flow*, 2nd ed. (Cambridge University Press, Cambridge, 1976).

[20] B. Bradshaw, Inactive motion and pressure fluctuations in turbulent boundary layers, J. Fluid Mech. **30**, 241 (1967).

[21] A. Lozano-Durán and J. Jiménez, Effect of the computational domain on direct simulations of turbulent channels up to $Re_\tau = 4200$, Phys. Fluids **26**, 011702 (2014).

[22] C. Chin, J. Monty, and A. Ooi, Reynolds number effects in DNS of pipe flow and comparison with channels and boundary layers, Int. J. Heat Fluid Flow **45**, 33 (2014).

[23] P. R. Spalart and J. H. Watmuff, Experimental and numerical study of a turbulent boundary layer with pressure gradients, J. Fluid Mech. **249**, 337 (1993).

[24] R. Johnstone, G. N. Coleman, and P. R. Spalart, The resilience of the logarithmic law to pressure gradients: Evidence from direct numerical simulation, J. Fluid Mech. **643**, 163 (2010).

[25] R. Zhao and A. Smits, Scaling of the wall-normal turbulence component in high-Reynolds-number pipe flow, J. Fluid Mech. **576**, 457 (2007).

[26] I. Marusic, J. P. Monty, M. Hultmark, and A. J. Smits, On the logarithmic region in wall turbulence, J. Fluid Mech. **716**, R3 (2013).

[27] V. Kulandaivelu, Evolution of zero pressure gradient turbulent boundary layers from different initial conditions, Ph.D. thesis, University of Melbourne, 2012.

[28] E. S. Winkel, J. M. Cutbirth, S. L. Ceccio, M. Perlin, and D. R. Dowling, Turbulence profiles from a smooth flat-plate turbulent boundary layer at high Reynolds number, Exp. Therm. Fluid Sci. **40**, 140 (2012).

[29] M. Hultmark, M. Vallikivi, S. C. C. Bailey, and A. J. Smits, Turbulent Pipe Flow at Extreme Reynolds Numbers, Phys. Rev. Lett. **108**, 094501 (2012).

[30] N. Hutchins, K. Chauhan, I. Marusic, J. P. Monty, and J. Klewicki, Towards reconciling the large-scale structure of turbulent boundary layers in the atmosphere and laboratory, Boundary-Layer Meteorol. **145**, 273 (2012).

[31] R. Örlü, T. Fiorini, A. Segalini, G. Bellani, A. Talamelli, and P. H. Alfredsson, Reynolds stress scaling in pipe flow turbulence - first results from CICLoPE, Philos. Trans. R. Soc. London, Ser. A **375**, 20160187 (2017).

[32] B. J. McKeon, J. Li, W. Jiang, J. Morrison, and A. J. Smits, Further observations on the mean velocity distribution in fully developed pipe flow, J. Fluid Mech. **501**, 135 (2004).

[33] P. R. Spalart and C. G. Speziale, A note on constraints in turbulence modelling, J. Fluid Mech. **391**, 373 (1999).

[34] B. Bradshaw (private communication).

[35] P. Luchini, An elementary example of contrasting laminar and turbulent flow physics, arXiv:1811.11877 [physics.flu-dyn].

[36] P. R. Spalart and S. R. Allmaras, A one-equation turbulence model for aerodynamic flows, La Recherche Aerospatiale **1**, 5 (1994).

[37] B. Eisfeld, C. Rumsey, and V. Togiti, Verification and validation of a second-moment-closure model, AIAA J. **54**, 1524 (2016).

[38] M. Mani, D. A. Babcock, C. M. Winkler, and P. R. Spalart, Predictions of a supersonic turbulent flow in a square duct, in *51st AIAA Aerospace Sciences Meeting including the New Horizons Forum and Aerospace Exposition*, Grapevine (Dallas/Ft. Worth Region), TX, 2013, AIAA Paper No. 2013-0860 (AIAA, Reston, VA, 2013).

[39] https://turbmodels.larc.nasa.gov.

[40] P. R. Spalart and S. R. Allmaras, A one-equation turbulence model for aerodynamic flows, in *30th Aerospace Sciences Meeting and Exhibit*, Reno, NV, 1992, AIAA Paper No. 92-0439 (AIAA, Reston, VA, 1992).

[41] T. Tsukahara, H. Kawamura, and K. Shingai, DNS of turbulent Couette flow with emphasis on the large-scale structure in the core region, J. Turbulence **7**, 1 (2006).

[42] S. Gandía-Barberá, S. Hoyas, M. Oberlack, and S. Kraheberger, The link between the Reynolds shear stress and the large structures of turbulent couette-Poiseuille flow, Phys. Fluids **30**, 041702 (2018).

[43] H. Abe, Direct numerical simulation of a non-equilibrium three-dimensional turbulent boundary layer over a flat plate, J. Fluid Mech. **902**, A20 (2020).

[44] J. Jiménez, S. Hoyas, M. P. Simens, and Y. Mizuno, Turbulent boundary layers and channels at moderate Reynolds numbers, J. Fluid Mech. **657**, 335 (2010).

[45] P. Schlatter and R. Örlü, Assessment of direct numerical simulation data of turbulent boundary layers, J. Fluid Mech. **659**, 116 (2010).

[46] A. Sillero, J. Jiménez, and R. Moser, One-point statistics for turbulent wall-bounded flows at Reynolds numbers up to $\delta^+ \approx 2000$, Phys. Fluids **25**, 105102 (2013).

[47] P. A. Monkewitz, Revisiting the quest for a universal log-law and the role of pressure gradient in "canonical" wall-bounded turbulent flows, Phys. Rev. Fluids **2**, 094602 (2017).

[48] X. Chen and K. R. Sreenivasan, Reynolds number scaling of the peak turbulence intensity in wall flows, J. Fluid Mech. **908**, R3 (2021).

[49] F. H. Clauser, The turbulent boundary layer, Adv. Appl. Mech. **4**, 1 (1956).

[50] T. Nakamura, T. Kameda, and S. Mochizuki, Effect of an adverse pressure gradient on the local similarity for a turbulent boundary layer, Trans. Jpn. Soc. Mech. Eng. Series B (in Japanese) **77**, 771 (2011).

[51] P. A. Monkewitz and H. M. Nagib, Large-Reynolds-number asymptotics of the streamwise normal stress in zero-pressure-gradient turbulent boundary layers, J. Fluid Mech. **783**, 474 (2015).